# Biologically bound nickel accelerated de-polymerization of polyethylene to high value hydrocarbons and hydrogen

Parul Johar[a], Elizabeth L. Rylott[b], C. Robert McElroy[a], Avtar S. Matharu[a], James H. Clark[a]*

*a Green Chemistry Centre of Excellence, Department of Chemistry, University of York, York, YO10 5DD, UK.*

*b Centre for Novel Agricultural Products, Department of Biology, University of York, Wentworth Way, York, YO10 5DD, UK*

*Correspondence:  james.clark@york.ac.uk*

This file includes:

Supplementary experimental section

Supplementary Figures (1-26)

Supplementary Tables (1-7)

**Experimental procedures**

Materials and chemicals

Two varieties of biomass were used in our experiments, the nickel (Ni) hyperaccumulator *Odontarrhena muralis* (previously *Alyssum murale)*, collected from fields on Ni-rich ultramafic soil, and hydroponically-grown willow (*Salix viminalis*) dosed with Ni. The dried plant biomass from these species was used for the preparation of phyto-catalyst (2.5 wt% and 0.1 wt% Ni respectively) along with a Ni-undosed willow controls (<0.01 wt% Ni). Willow rods were grown hydroponically for six weeks using the Aeroflo system (General Hydroponics) then dosed with 100 mg $L^{-1}$ of $NiNO_3.6H_2O$ (Sigma Aldrich) solution for two weeks (Fig.1).[1] Metal accumulation was determined in leaves and stems using an inductively coupled plasma optical emission spectrometer (ICP-OES, Agilent 700 series.

The low-density polyethylene (LDPE) used in this study was purchased from Sigma Aldrich. The $M_n$ and $M_w$ of LDPE are $1.700 \times 10^3$ and $4.000 \times 10^3$, respectively, measured by GPC. All other chemicals were purchased from Sigma-Aldrich and were used as received unless otherwise stated.

Catalysts preparation and characterization

The catalyst was prepared using the method described previously.[1] Firstly, microwave assisted pyrolysis on air-dried, ground leaf tissues from the plant species was performed on a CEM Discover, equipped with 30 ml quartz vial under $N_2$ at 250 °C and 200 W to produce bio-char with different Ni-loadings (termed as phytocat). The feedstock was converted into vapors, which were passed through a condenser and collected as liquid oil. The mass yield of bio-char and bio-oil produced were measured and the gas yield calculated as the mass balance of the original sample. The total conversion was evaluated based on the sum total of liquid and gas yields. After the extraction of bio oil and biogas, the biochar containing naturally bound Ni with different metallic loadings was used as catalyst.

The thermal decomposition profiles were monitored using the thermo-gravimetric analysis with Fourier transform infrared (TGA-IR) analysis in the temperature range of

30 °C to 700 °C at a heating rate of 10 °C min$^{-1}$ under nitrogen atmosphere of 100 ml min$^{-1}$ flow rate (Fig.S5). The analysis was done using the plant biomass (with and without Ni). The TG-IR was carried out using a Netsch STA409 linked to a gas cell in a Bruker Equinox 55 infra-red spectrometer by a heated gas line. The volatiles released during pyrolysis were immediately transferred to the FTIR gas cell and analyzed using a FTIR equipped with an MCT detector within the range of 500–4000 cm$^{-1}$ at a resolution of 4 cm$^{-1}$. The thermal stability of produced carbon on the spent catalyst was studied by the temperature-programmed oxidation (TPO) process using a Netsch STA409 thermo-gravimetric analyzer (TGA). The oxidation process started from heating to 700 °C at a heating rate of 10 °C/min in an air atmosphere and holding at 700 °C for another 10 min.

High-angle annular dark-field -scanning transmission electron microscope (HAADF-AC-STEM) images were acquired using a 200 keV JEOL 2200FS scanning transmission electron microscope with a field emission gun. Sample preparation for TEM analysis was done by crushing a few grains of the sample between two microscope glass slides and dusting with powder holey carbon films supported by 300 mesh TEM Cu grids (Agar scientific, S147-3). Excess powder was then removed by flicking the grids onto the edges of the glass slides under a fume hood before transfer to single tilt TEM sample holders.

Transmission electron microscopy (TEM, JEOL 2010) was used under the accelerating voltage of 200 kV to investigate the microstructure of phytocat material. The TEM samples were prepared by suspending in methanol, followed by sonication for 10 minutes. A uniform thin layer of the sample was deposited on a carbon grid support followed by air-drying. Microstructural and chemical information of phytocat was obtained by using a field-emission scanning electron microscope (FE-SEM) equipped with an energy-dispersive X-ray (EDX) spectrometer (JSM-7800F PRIME, JEOL Ltd.). Elemental composition and valence near the surface were measured using XPS (AXIS Ultra DLD, Kratos. Inc.), and the data were analyzed using CASA XPS software. Fourier-Transform Infrared Spectroscopy (FTIR) characterized surface functional groups of the pristine and recycled catalysts. Background scans were conducted before each sample was scanned. Samples were placed in ATR crystal and

scanned in the wavelength range of 600–4000 cm$^{-1}$. The XRD was performed at operating voltage of 40 kV, current, 40 mA, scan speed of 0.1 sec/step and the scan scope from 10 $\Theta$ to 90 $\Theta$ using a Bruker AXS D8 Advance. Further, Ni particle size was estimated using the Scherrer equation using the peak centered at $2\theta= 44.5°$.

$N_2$ adsorption–desorption analysis was performed at 77 K using a TriStar (Micromeritics Instrument Corp.; Norcross, GA, USA), equipped with automated surface area and pore size analyser. Before analysis, samples were degassed at 180 °C for 4 h (Fig.S6).

Conventional thermal and microwave-assisted de-polymerization of polyethylene

The phytocat produced using microwave pyrolysis was then mixed with PE to produce mixtures (1:1, 1:2, 1:5, 1:10 and 1:20) by weight. Microwave pyrolysis of these mixtures (1g each) was performed on CEM Discover, equipped with 30 mL quartz vial at 250 ℃ and 200 W. The mass yields of biochar and pyrolysis oil produced were measured after every microwave run (up to 3 consecutive microwave runs) and the gas yield calculated as the mass balance of the original sample. The total conversion was evaluated based on the sum total of liquid and gas yields. Further, the de-polymerization efficiency of the phytocat materials was calculated based on the percentage conversion of polyethylene into de-polymerized products. The evolved gas was trapped using syringes (1 mL volume, Series A-2 pressure-lok precision analytical gas syringe) for qualitative analysis. The control experiments were carried out using willow bio-char without Ni (termed as control phytocat) and activated carbon. All the experiments were performed in triplicates.

The conventional study to monitor de-polymerization of LDPE was done using the simultaneous thermal analyzer with gas chromatography equipped with mass spectrometry (TG-GC-MS, Netzsch STA 449) profiles in the temperature range of 30 °C to 650 °C at a heating rate of 10 °C min$^{-1}$ under under He. The analysis was performed using the phytocat materials or activated carbon and polyethylene mixtures (1:10 by weight).

Stability of the phytocat

The phytocat materials post microwave-assisted de-polymerization of LDPE were recovered and re-used for the consecutive de-polymerization experiments at a catalyst to polymer ratio of 1:10 by weight under the same conditions as mentioned above. Briefly, microwave-assisted pyrolysis of these mixtures (1g each) was performed on a CEM Discover, equipped with 30 mL quartz vial at 250 ℃ and 200 W. The mass yields of biochar and pyrolysis oil produced were measured after every microwave run (up to 3 consecutive microwave runs for all catalysts and for 6 consecutive runs using the best performing catalyst i.e. phytocat-2.5) and the gas yield calculated as the mass balance of the original sample. The total conversion was evaluated based on the sum total of liquid and gas yields (see Figure S19).

Furthermore, the recovered catalysts were analyzed using the above-mentioned material characterization techniques. The thermal stability of recovered catalyst was investigated using temperature-programmed oxidation (TPO) process on a Netsch STA409 thermo-gravimetric analyzer (TGA). The oxidation process started from heating to 700 °C at a heating rate of 10 °C/min in an air atmosphere and holding at 700 °C for another 10 min. Moreover, the thermal stability was investigated using thermo-gravimetric analysis (TGA, Netzsch STA 449) profiles in the temperature range of 30 °C to 650 °C at a heating rate of 10 °C min$^{-1}$ under He. The analysis was performed using the recovered phytocat-2.5 and polyethylene mixtures (1:10 by weight) after every successive run (see Figures S21-26).

Additionally, the experiments were conducted to demonstrate catalyst longevity and deactivation for up to 6 successive runs using our best catalyst (phytocat-2.5). The study was extended to understand coking effects and therefore, quantitative characterization of products yield was performed (see Supplementary Table 2) alongside the material characterization tests of the recovered catalyst (see Figure S4).

Qualitative analysis of de-polymerization products

Gas chromatography coupled with mass spectrometry, GC–MS (JEOL AccuTOF-GCx plus, Agilent 7890B GC) was used for analysis of liquid products. The column used was Phenomenex ZB-5MSplus (30m x 0.25 mm id x 0.25um film thickness) with film composition of 5% Phenyl-Arylene, 95% dimethylpolysiloxane. The column oven was initially held at 45 °C for 1 min followed by a ramp at the rate of 5 °C min⁻¹ to 300 °C, and finally held at this temperature for 10 min to allow elution of all the compounds. The constituents of samples were identified by comparing the mass spectra with national institute of standards and technology (NIST) research library. Relative content of each compound was measured by semi-quantitative method by calculating the chromatographic peak area (Supplementary Tables 2-10).

The qualitative analysis of gas was performed using an Agilent Technologies 7820A gas chromatograph, with a flame ionization detector (GC-FID), fitted with a Carboxen 1010 PLOT 30m x 0.53mm capillary column. Argon was used as the carrier gas at a flow rate of 2 mL/min with a split ratio of 10:1 and a 1mL injection. The initial oven temperature was 100°C (held for 2 minutes) and was increased at a rate of 25°C/min to 250°C and held at this temperature for 20 minutes, with a total run time of 28 minutes. Injection temperature was 200°C and the detector temperature was 250°C.

Product yields and energy consumption analysis

Product yields are expressed as per cent by weight of dry feed. The liquid and solid fractions were measured by weighing. Gas fraction mass was estimated by the difference between initial sample mass and sum of solid residue and liquid product mass.

Conversion (%) = $\dfrac{Wi - Wr}{Wi} \times$ 100…………………………………………………..(1)

Yield of oil (%) = $\dfrac{Wo}{Wi} \times$ 100……………………………………………………(2)

Yield of residue (%) = $\dfrac{Wr}{Wi} \times$ 100…………………………………………….(3)

Yield of gas (%) = $100 -$ (yield of oil + yield of residue)…………………………………………………………………………..(4)

Here, $W_i$, $W_o$ and $W_r$ are defined as initial weight of LDPE, weight of oil produced by microwave assisted pyrolysis of LDPE and weight of solid residue after reaction, respectively.

The energy consumption analysis of MW assisted de-polymerization process was done in terms of energy consumption to pyrolyze unit g of feed to reach the set-point of T= 250 °C at fixed MW power of 200 W, using the following equation

$$\text{Energy consumption (KJ/g)} = \frac{P\ (W) \times t\ (s)}{Amount\ of\ feed-stock\ (g)} \quad\text{..........................(5)}$$

The qualitative and the quantitative analysis of the products formed by microwave-assisted de-polymerization of LDPE using phytocat materials was conducted after every successive microwave cycle in order to investigate the stability and performance of the phytocat (see supplementary Tables 2-6).
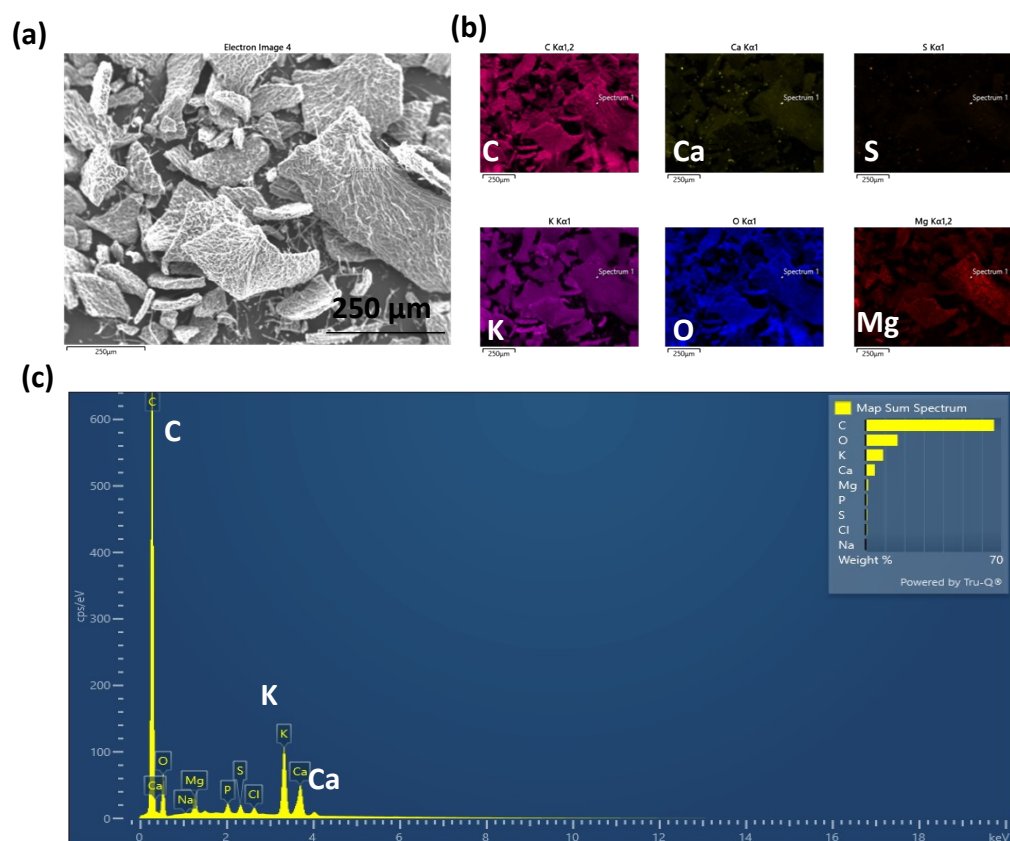
Figure S1: (a) Scanning electron microscopy (SEM) images equipped with energy-dispersive X-ray spectroscopy (EDX) analysis of control phytocat, (b) Elemental mapping of control phytocat highlighting carbon, calcium, sulfur, potassium, oxygen and magnesium, (c) The EDX spectroscopy analysis of control phytocat.
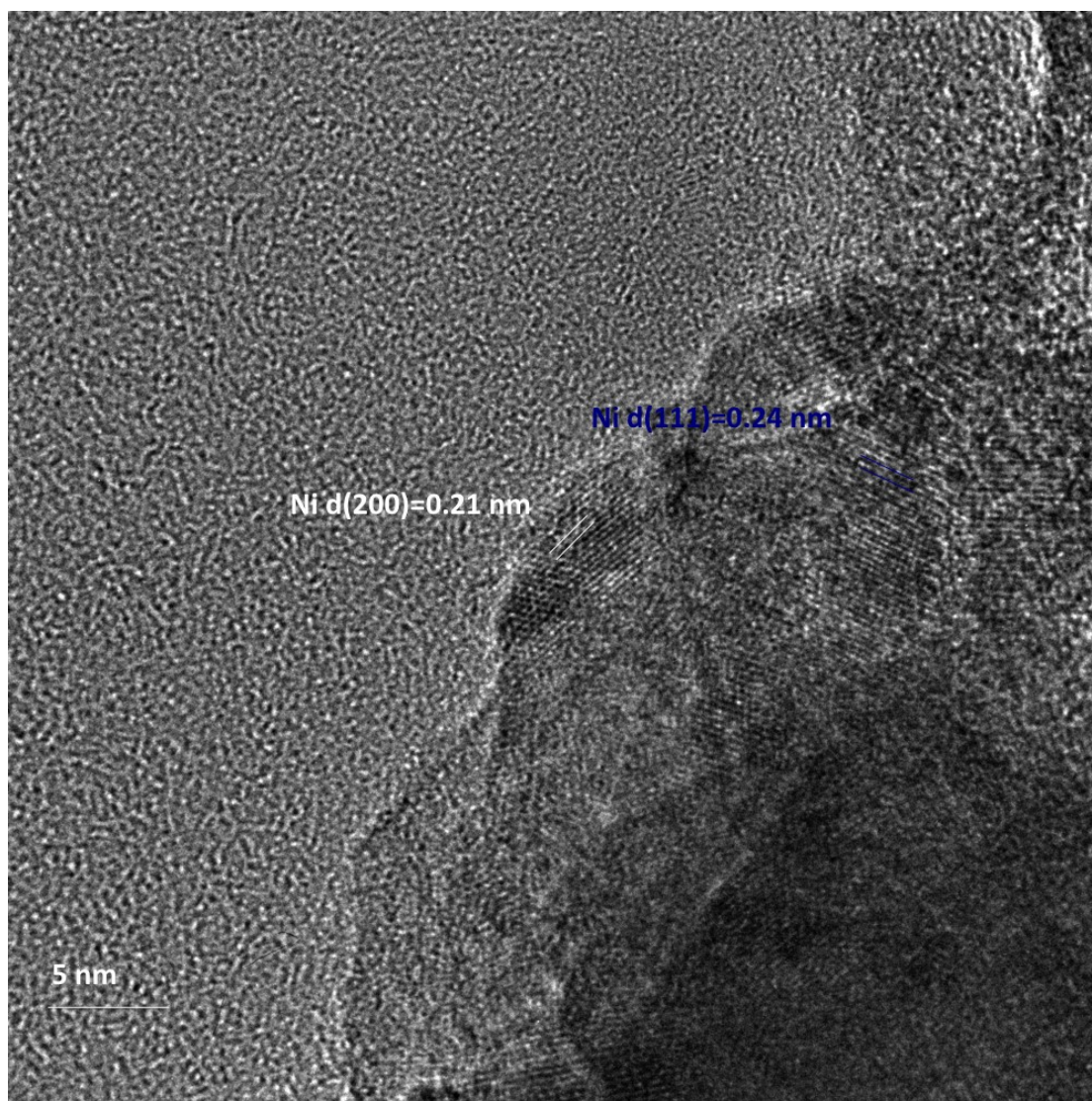
Figure S2: High-resolution TEM (HRTEM) image of Ni-phytocat-2.5 showing lattice fringes corresponding to (111) and (200) crystal planes, respectively, of cubic Ni phase.
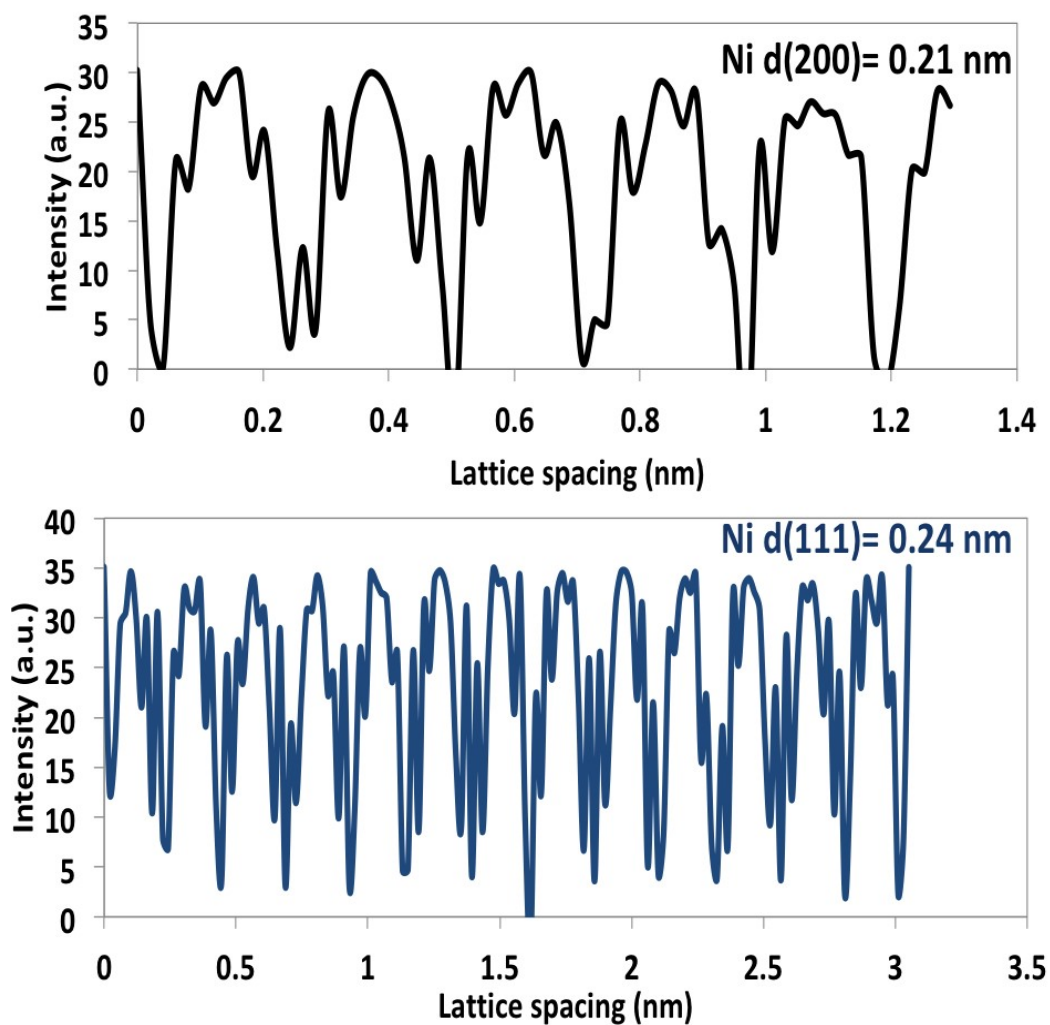
Figure S3: Plots of lattice spacing corresponding to the fast fourier transform (FFT) pattern of the high-resolution TEM (HRTEM) image of Ni-phytocat-2.5
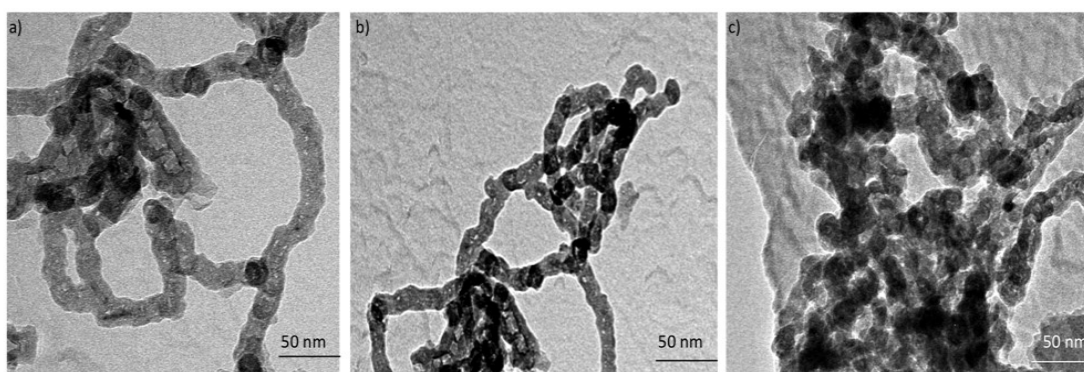
Figure S4: High-resolution TEM (HRTEM) image of the recovered Ni-phytocat-2.5 after (a) 1st successive run and (b) 3rd successive run and (c) 6th successive run.
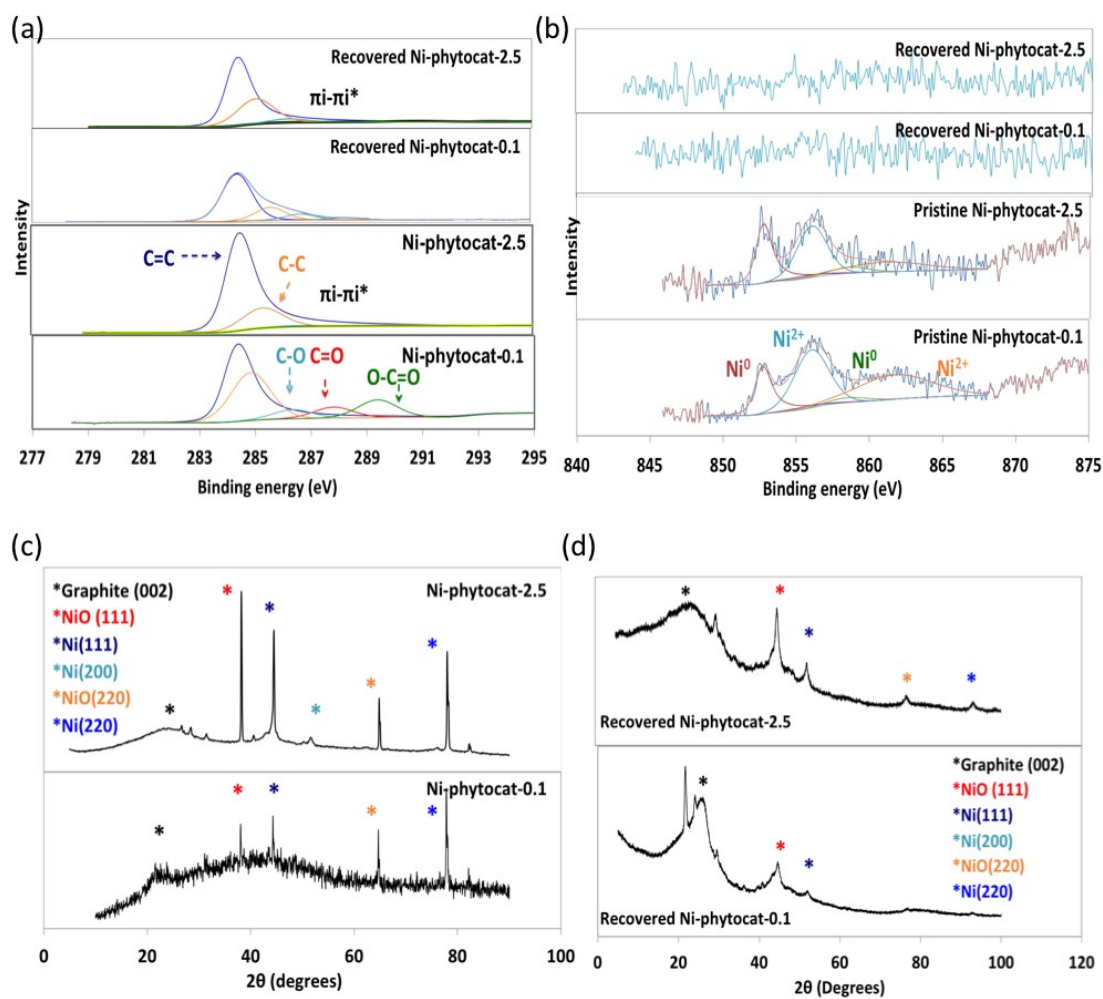
Figure S5: X-ray photoelectron spectroscopy (XPS) analysis of phytocat materials
(a) deconvoluted high-resolution C 1s spectra (b) deconvoluted high-resolution Ni $2p_{3/2}$ spectra , (c) X-ray diffraction (XRD) pattern of Ni-phytocat-2.5 and -0.1, (d) XRD pattern of recovered Ni-phytocat-2.5 and -0.1.
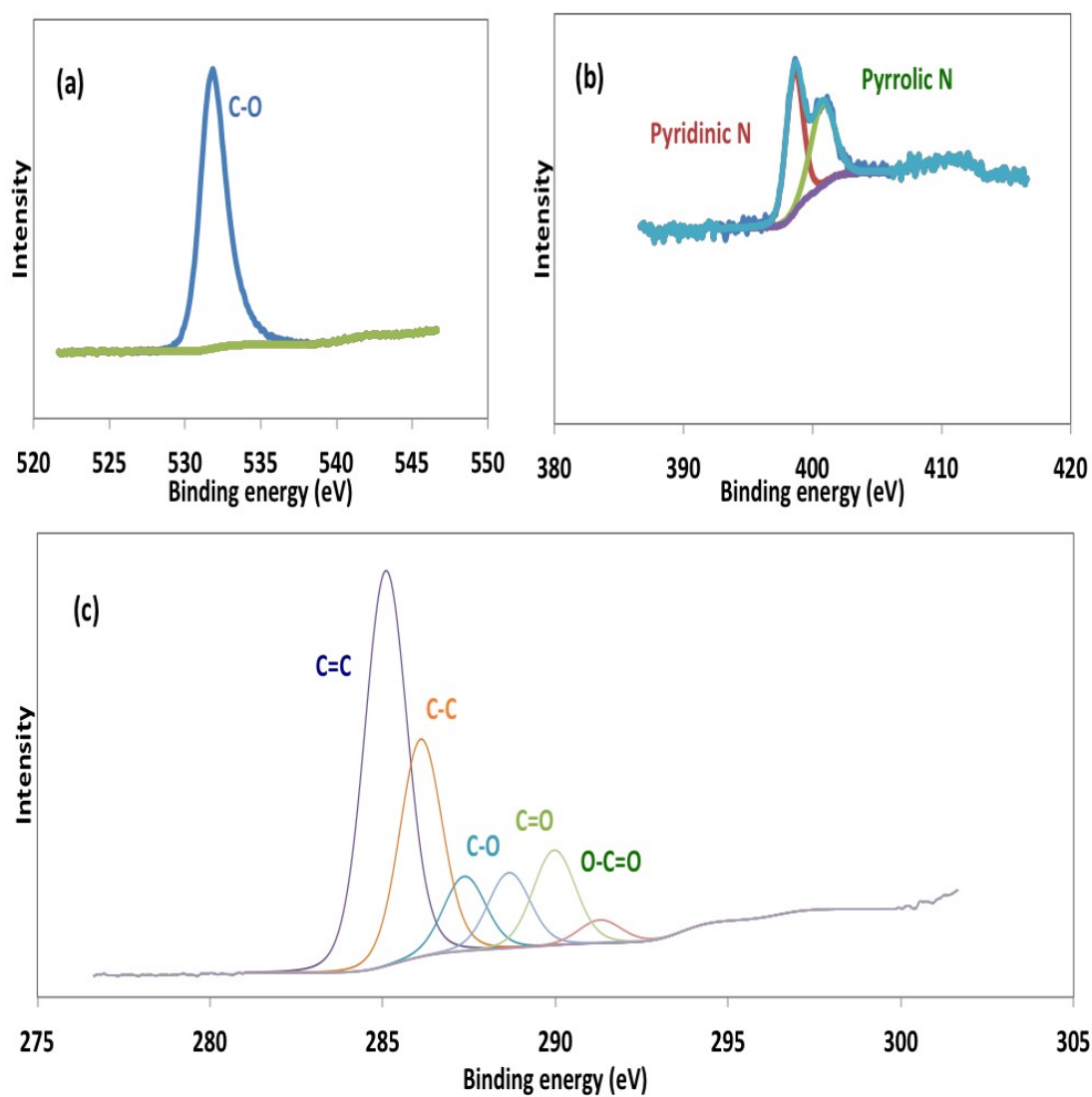
Figure S6: X-ray photoelectron spectroscopy (XPS) analysis of control phytocat
(a) deconvoluted high-resolution O 1s spectra, (b) deconvoluted high-resolution N 1s
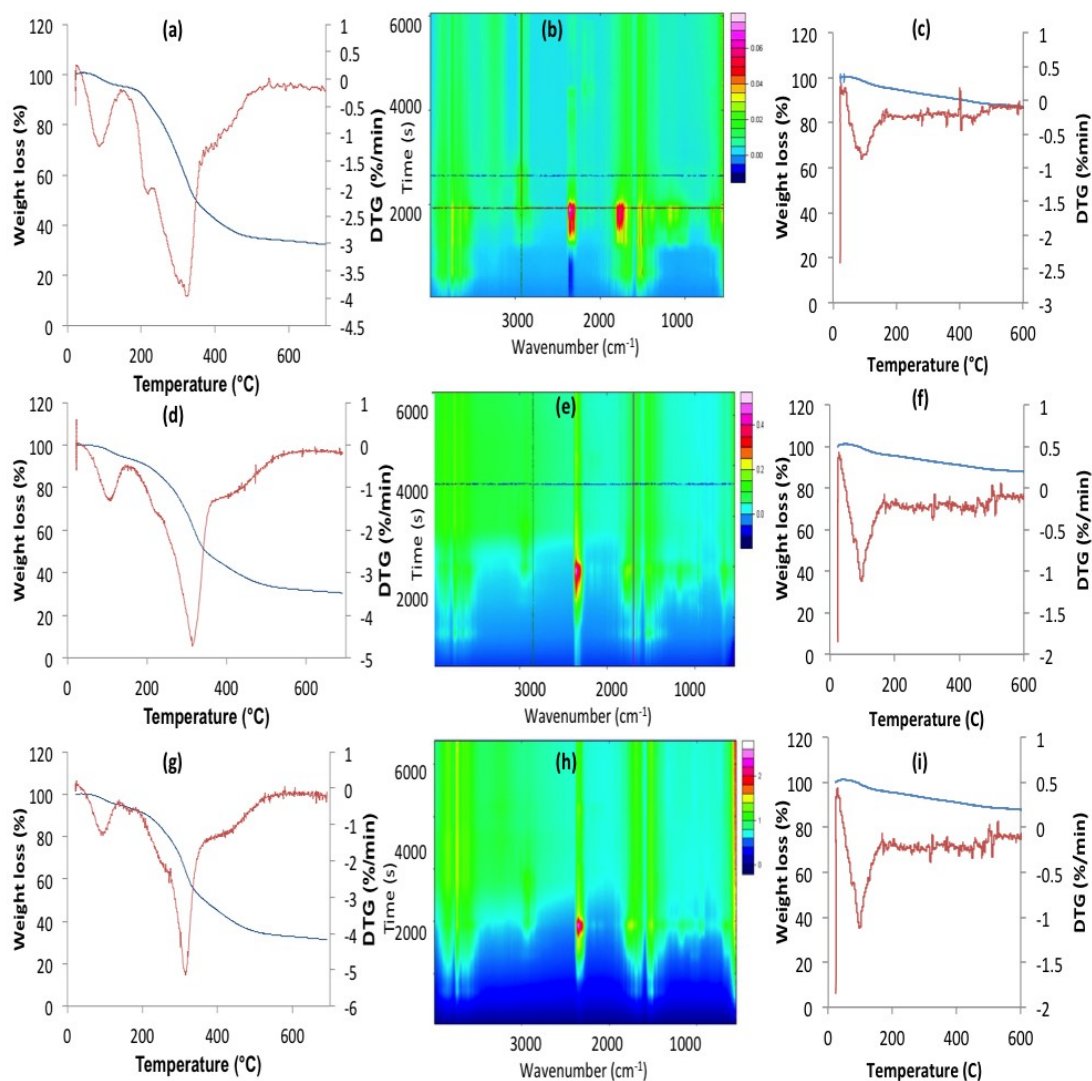spectra, (c) deconvoluted high-resolution C 1s spectra.

Figure S7: Real time thermogravimetric analysis coupled with fourier transform infrared spectroscopy (TGA-FTIR) for functional groups analysis of evolved gases in real-time for (a-b) *Odontarrhena muralis* (previously *Alyssum murale)* biomass pre-pyrolysis, (c) Ni-phytocat-2.5, (d-e) Ni-dosed willow biomass pre-pyrolysis (f) Ni-phytocat-0.1, (g-h) undosed willow biomass pre-pyrolysis (i) control phytocat .
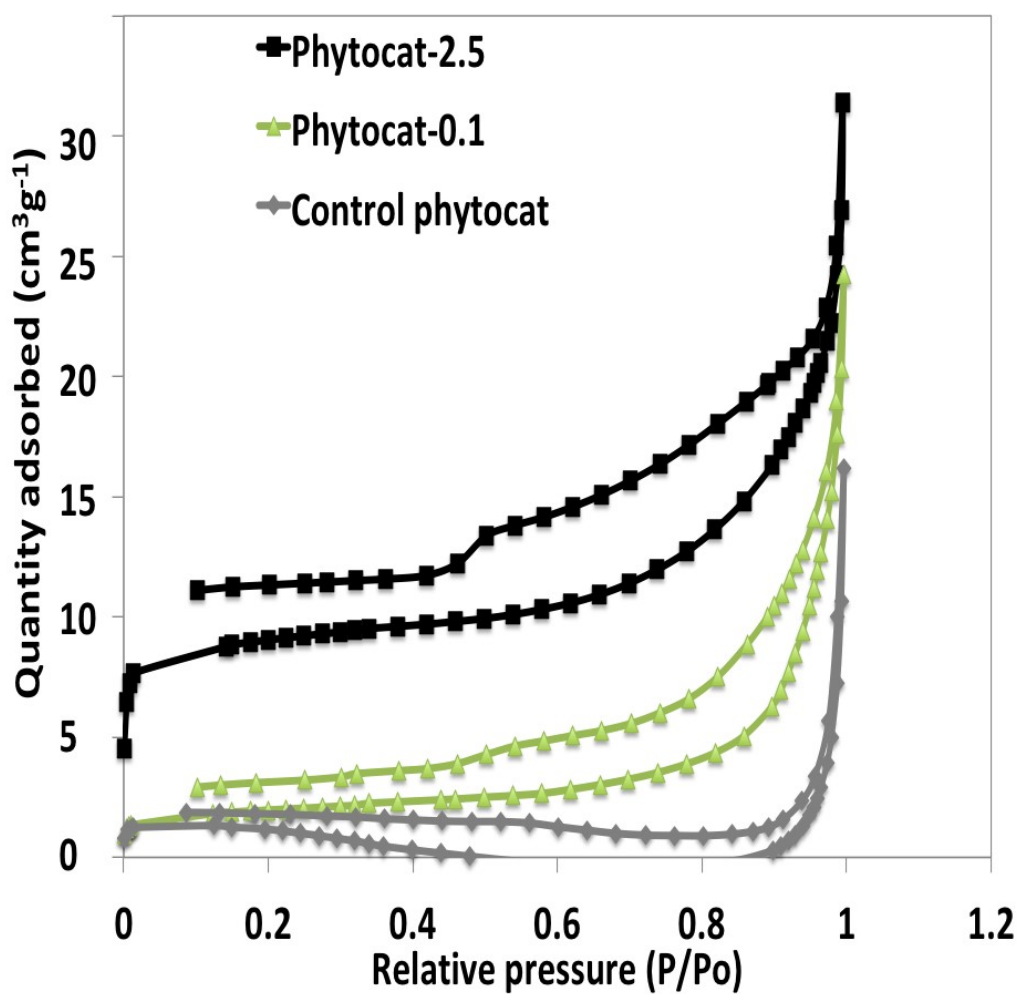
Figure S8: Adsorption/desorption isotherms of $N_2$ at 77 K of phytocat materials
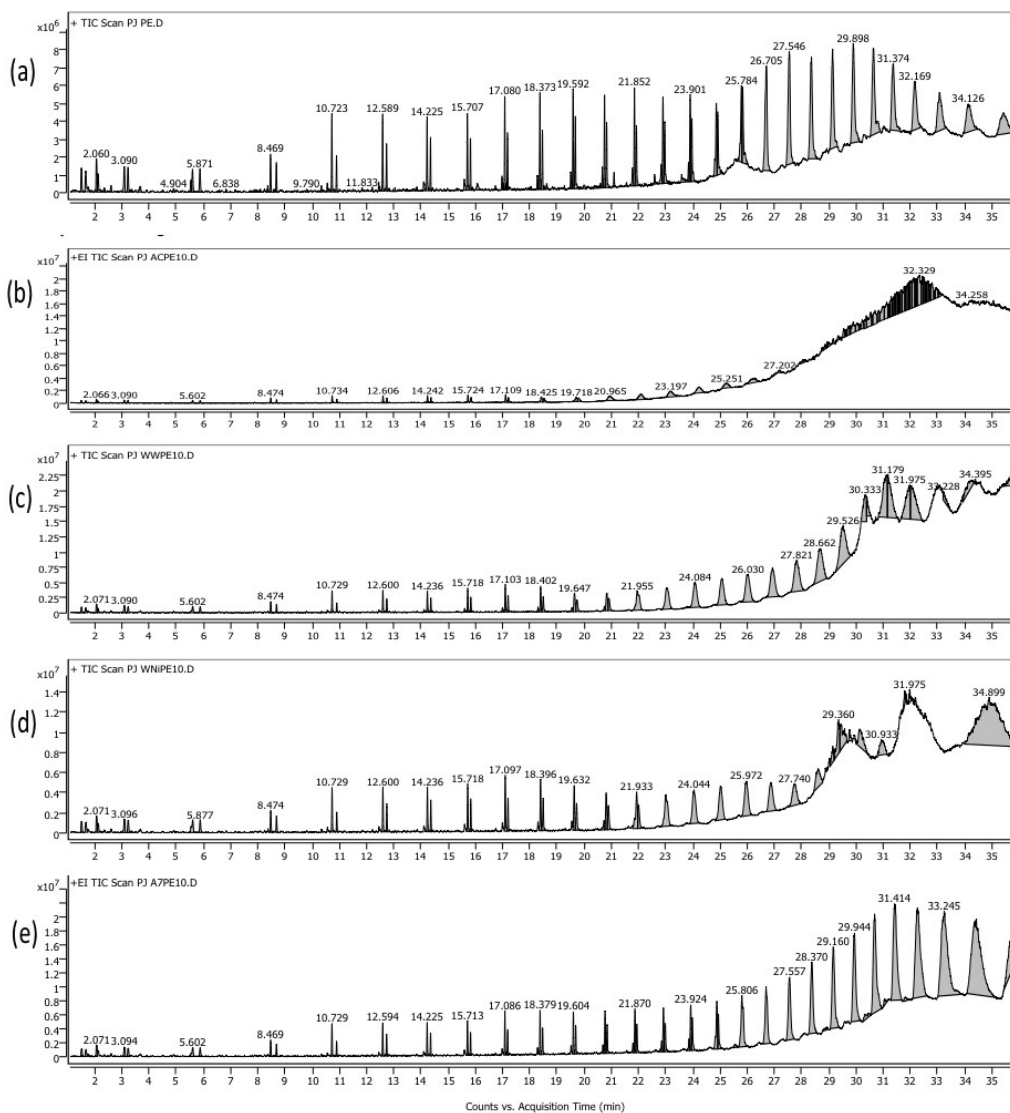
Figure S9: Gas chromatograms of the pyrolysis oils produced using conventional pyrolysis of (a) low density polyethylene (LDPE), (b) activated carbon: LDPE, (c) control phytocat: LDPE, (d) phytocat-0.1: LDPE and (e) phytocat-2.5: LDPE (1:10 by weight)
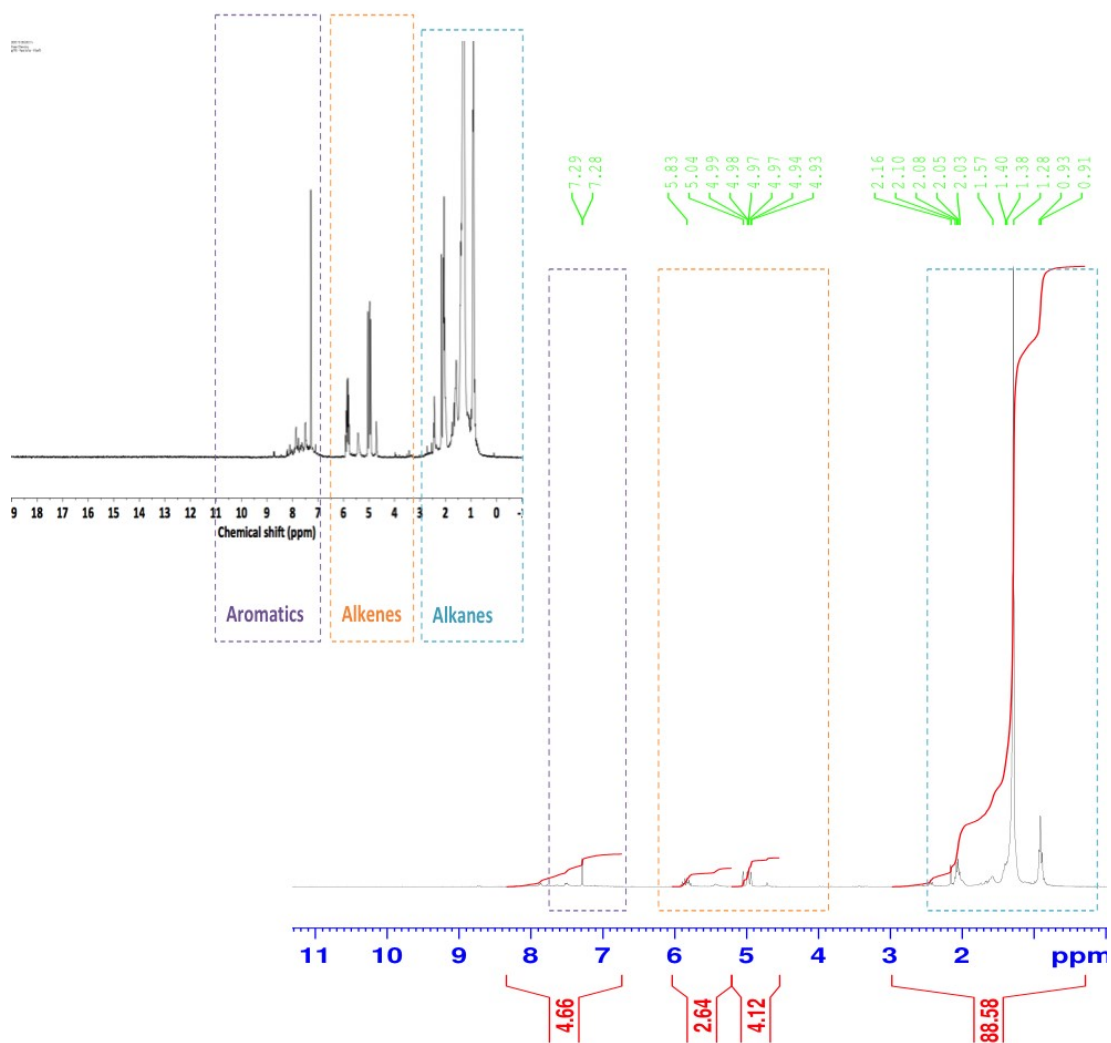
Figure S10: ^{1}HNMR analysis of the oil formed after microwave assisted depolymerization of LDPE using Ni-phytocat-2.5
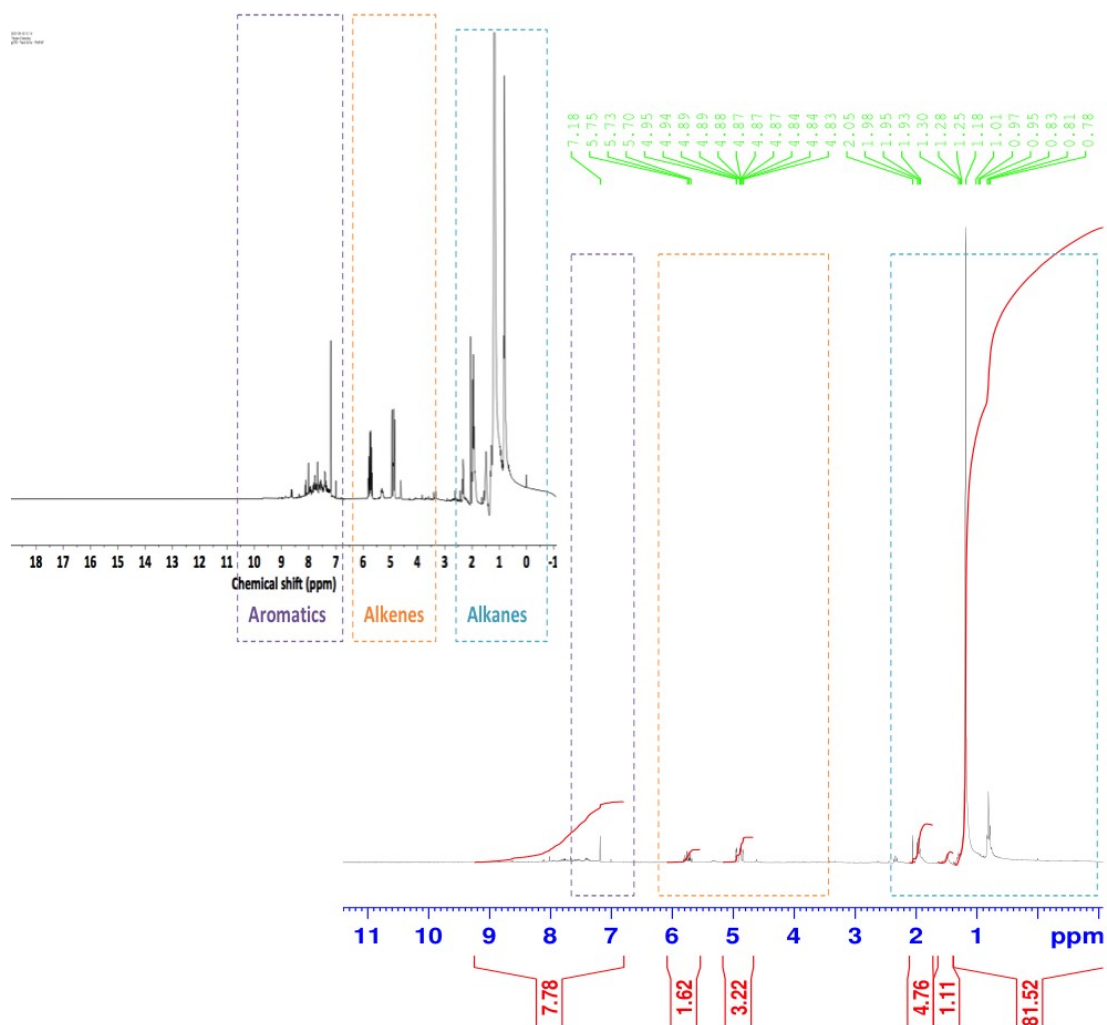
Figure S11: ^{1}HNMR analysis of the oil formed after microwave assisted de-polymerization of LDPE using Ni-phytocat-0.1
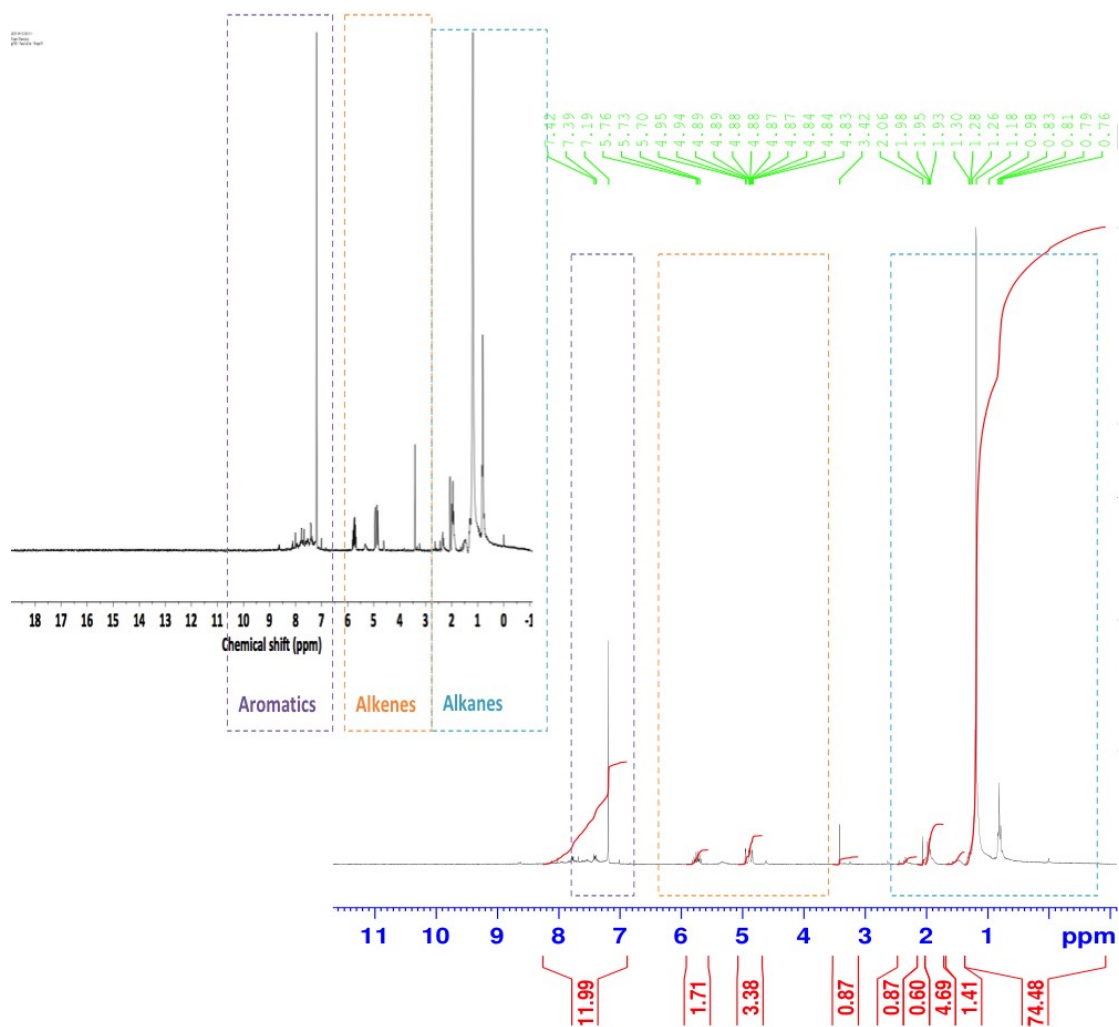
Figure S12: ¹HNMR analysis of the oil formed after microwave assisted de-polymerization of LDPE using control-phytocat
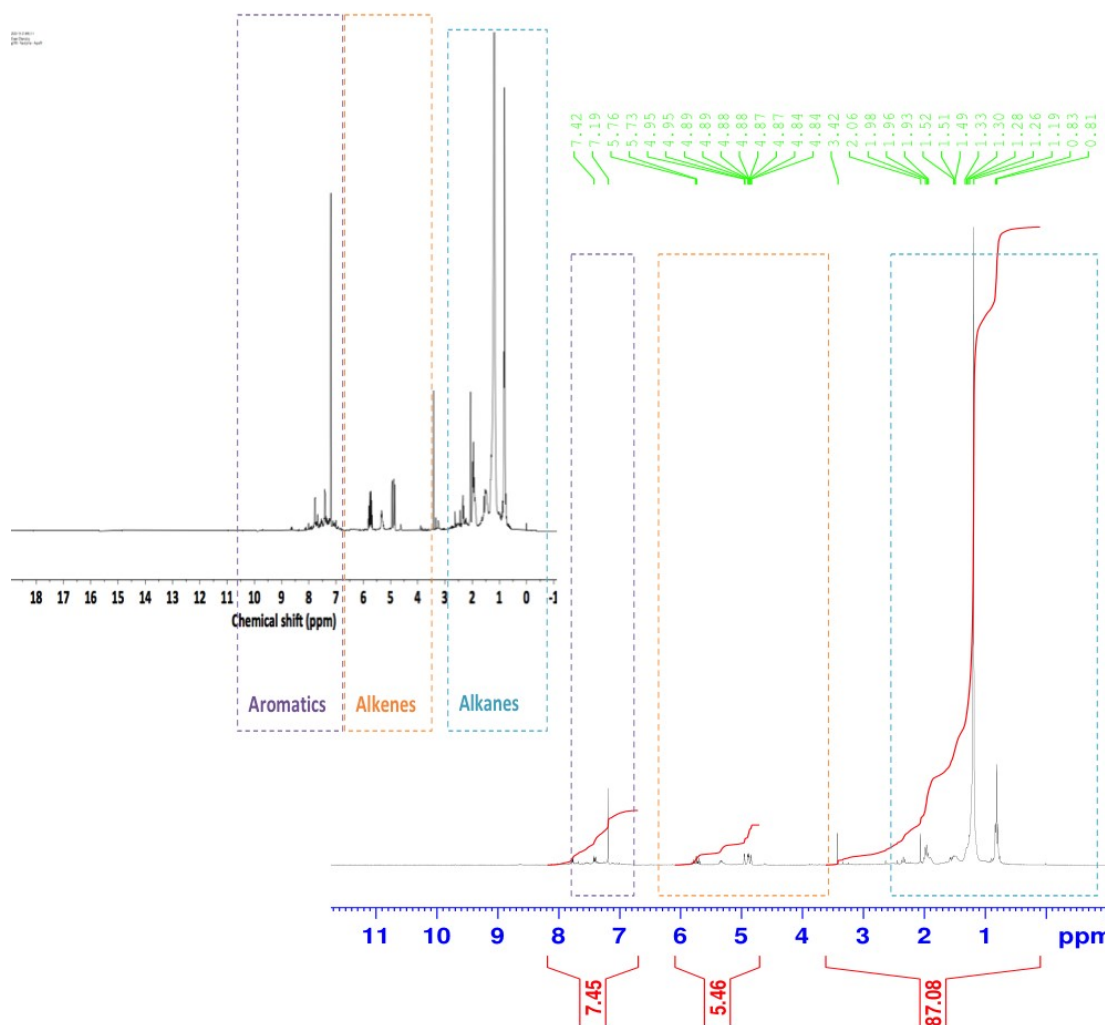
Figure S13: ¹HNMR analysis of the oil formed after microwave assisted de-polymerization of LDPE using activated carbon

Figure S14: GC-MS chromatogram of the pyrolysis oil produced by the microwave-assisted pyrolysis of LDPE using phytocat-2.5
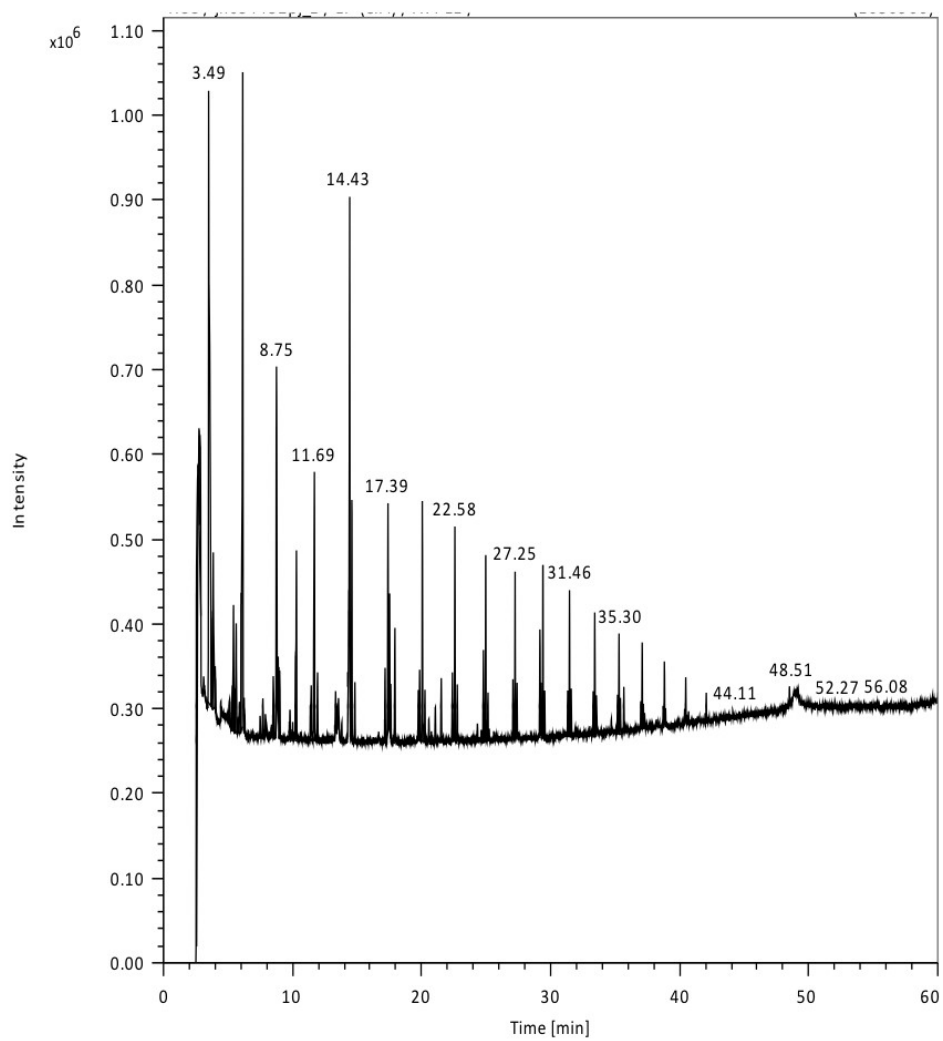
Figure S15: GC-MS chromatogram of the pyrolysis oil produced by the microwave-assisted pyrolysis of LDPE using phytocat-0.1
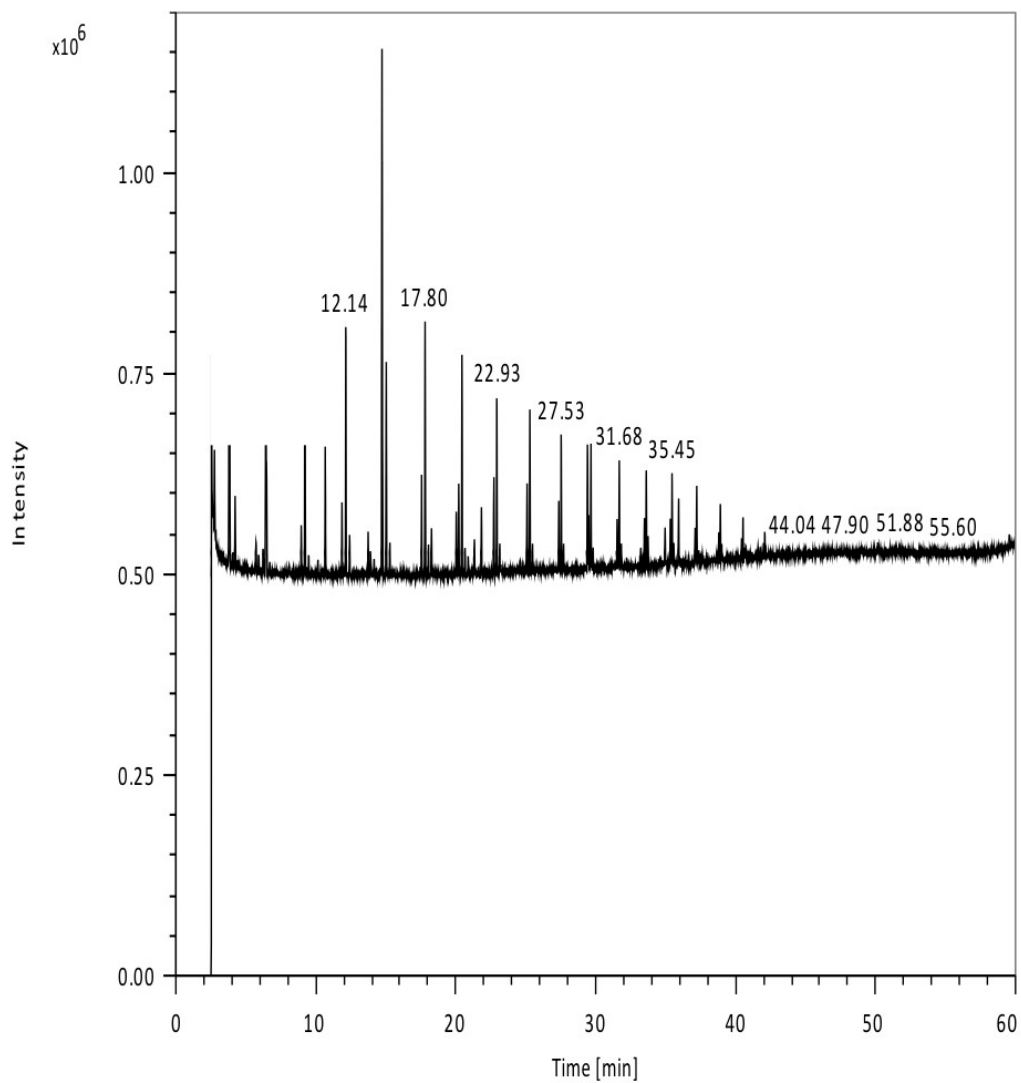
Figure S16: GC-MS chromatogram of the pyrolysis oil produced by the microwave-assisted pyrolysis of LDPE using control phytocat
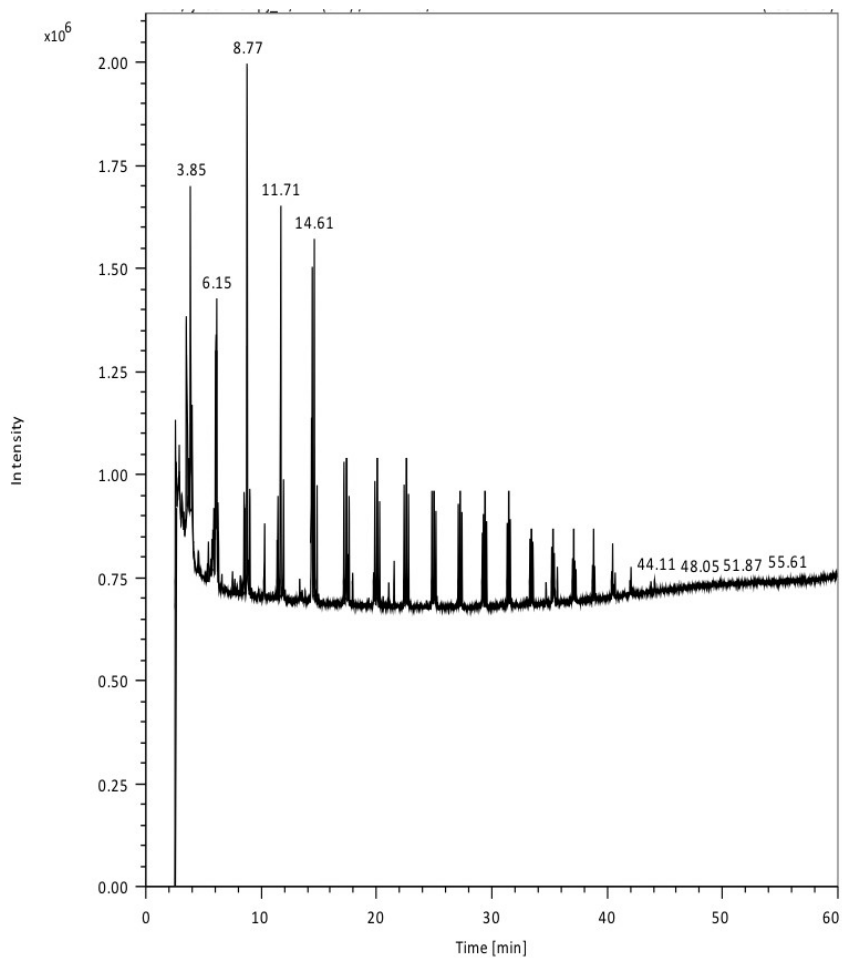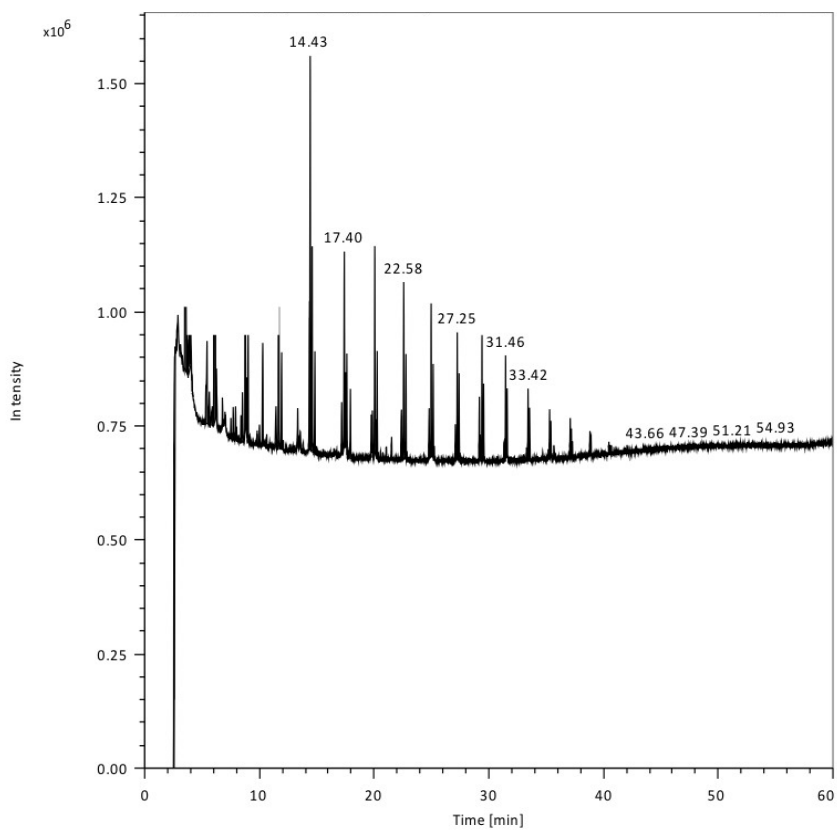
Figure S17: GC-MS chromatogram of the pyrolysis oil produced by the microwave-assisted pyrolysis of LDPE using activated carbon
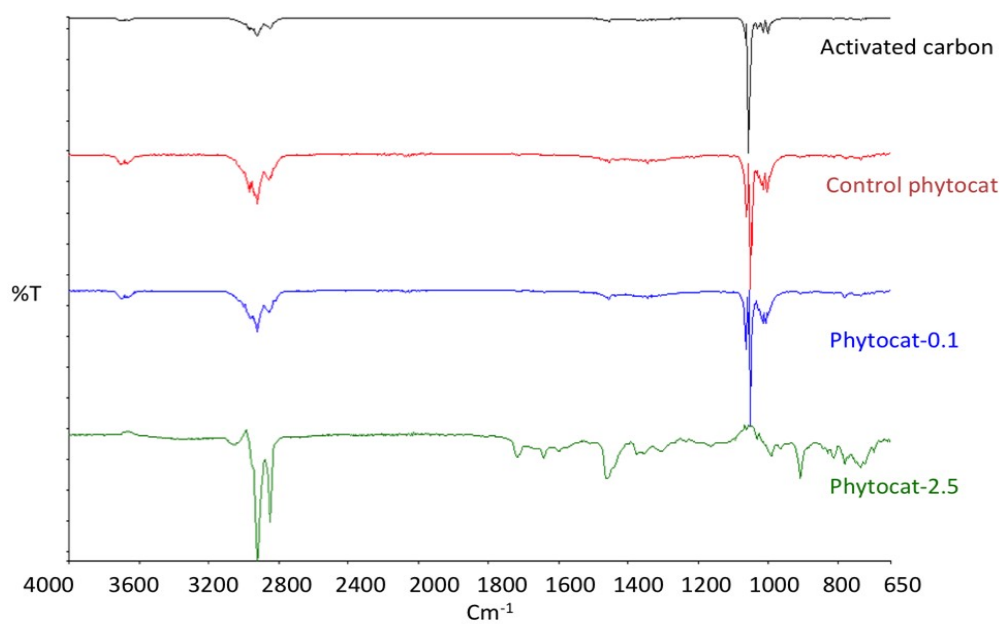
Figure S18: FTIR spectra of the oils produced by microwave-assisted pyrolysis of LDPE using various catalysts (1:10 catalyst to polymer ratio by weight)
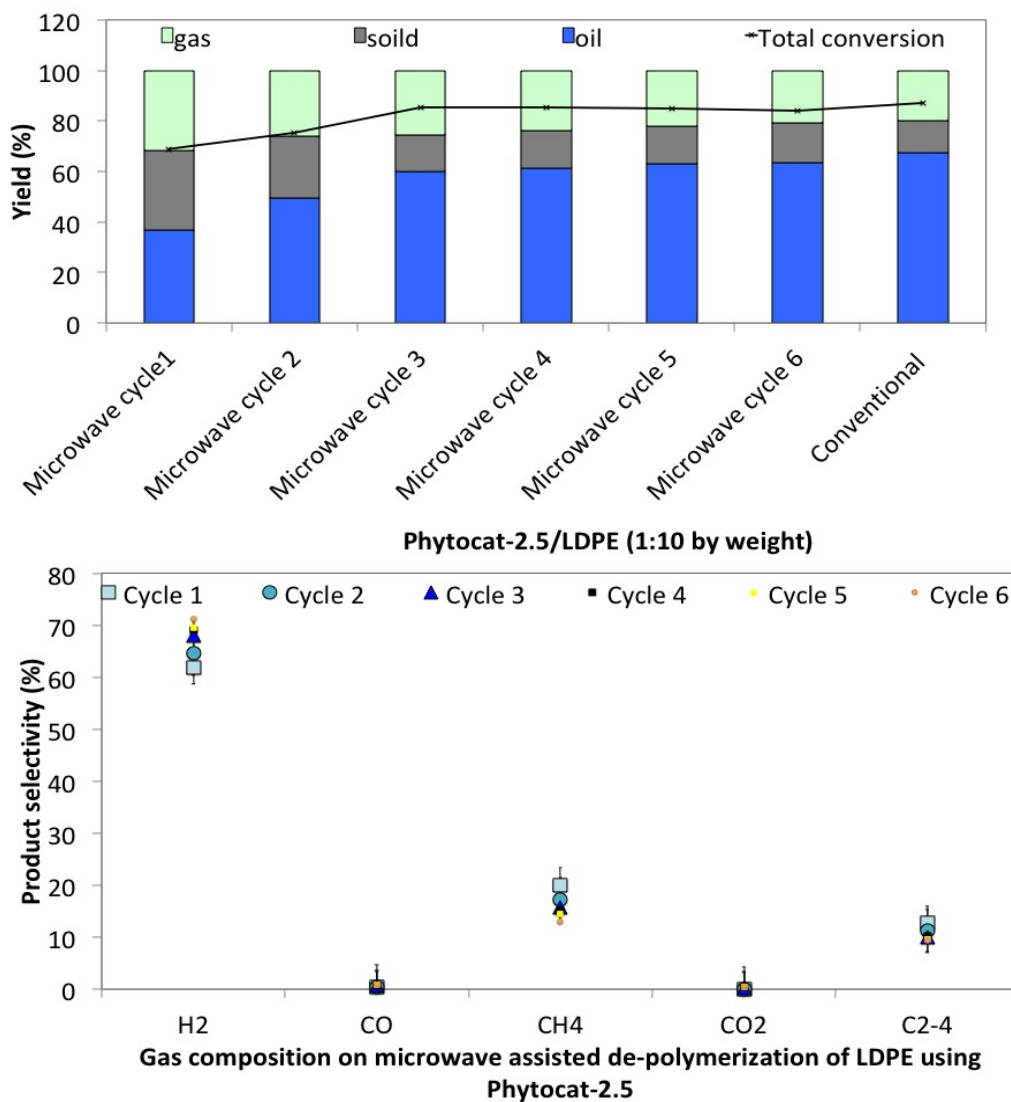
Figure S19: Performance of phytocat-2.5 for successive microwave- assisted de-polymerization of LDPE
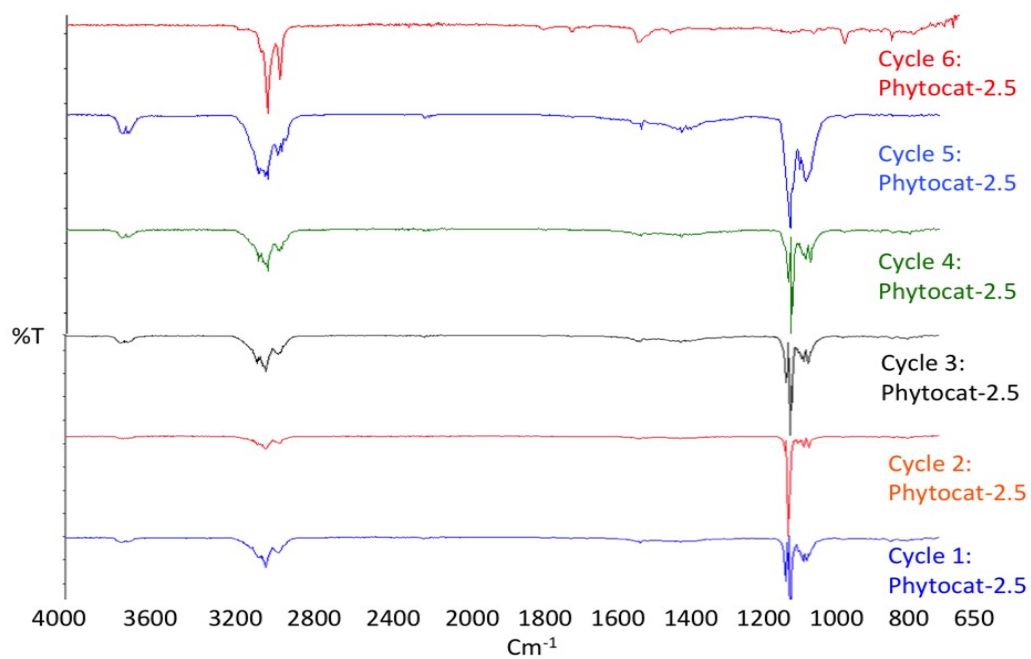
Figure S20: FTIR spectra of the oils produced by microwave-assisted pyrolysis of LDPE using phytocat-2.5 (1:10 catalyst to polymer ratio by weight) for 6 consecutive cycles
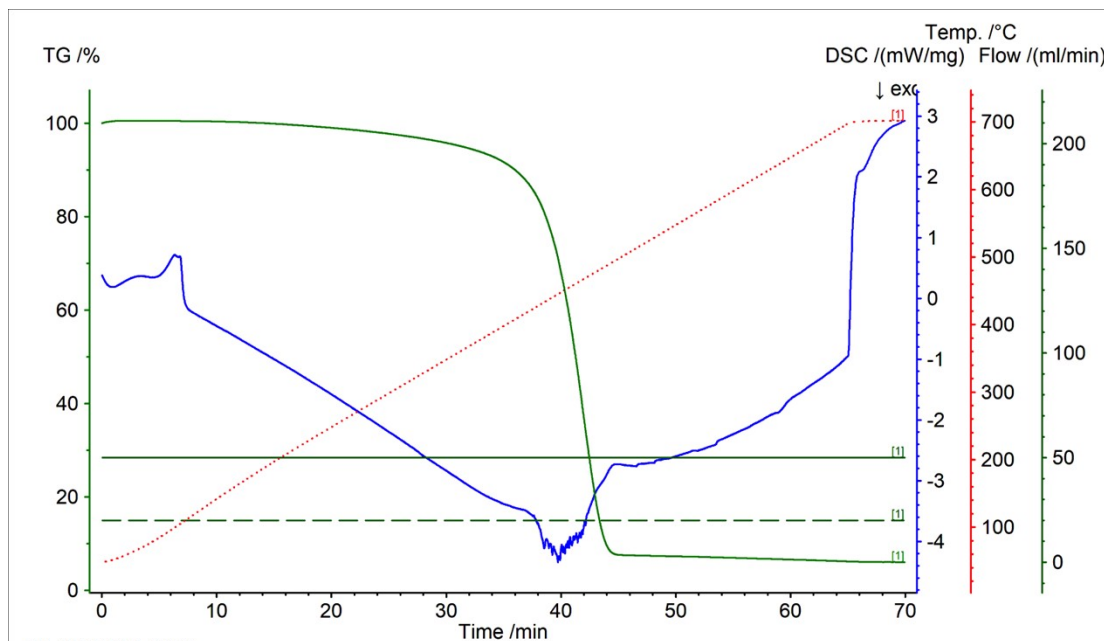
Figure S21: Thermo-gravimetric analysis (TGA) profile of the mixture of phytocat-2.5 and LDPE (1:10 by weight, Cycle 1)
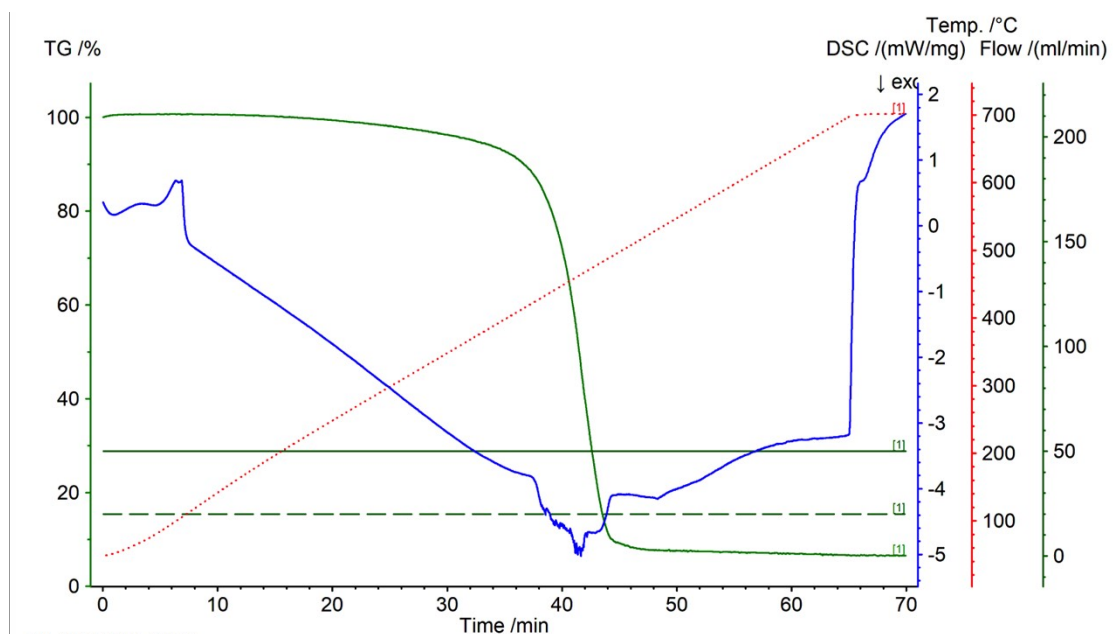
Figure S22: Thermo-gravimetric analysis (TGA) profile of the mixture of phytocat-2.5 and LDPE (1:10 by weight, Cycle 2)
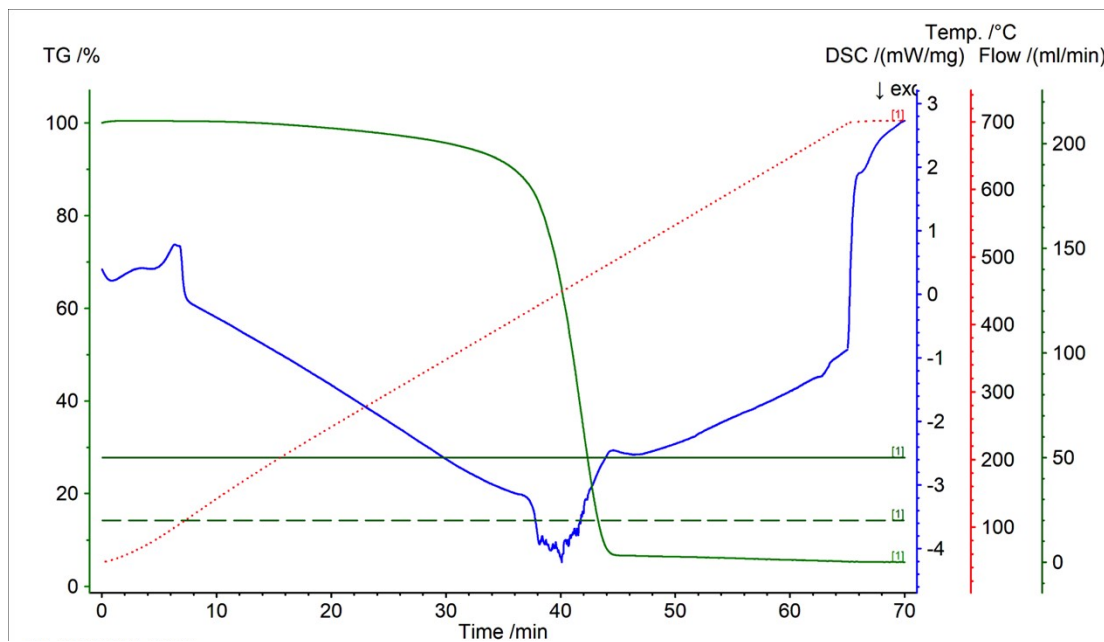
Figure S23: Thermo-gravimetric analysis (TGA) profile of the mixture of phytocat-2.5 and LDPE (1:10 by weight, Cycle 3)
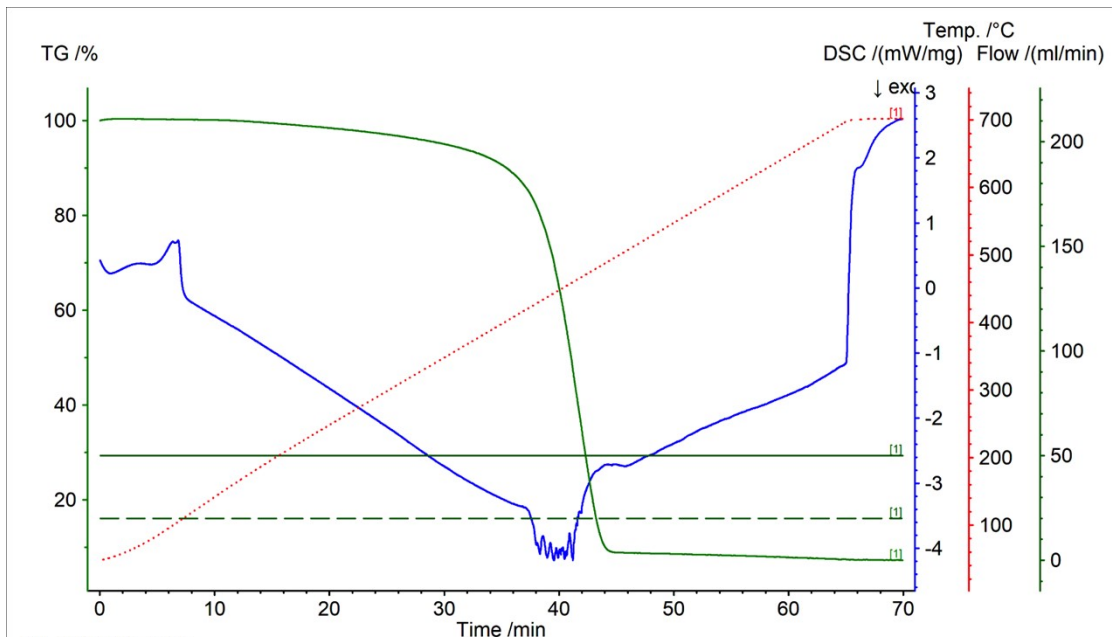
Figure S24: Thermo-gravimetric analysis (TGA) profile of the mixture of phytocat-2.5 and LDPE (1:10 by weight, Cycle 4)
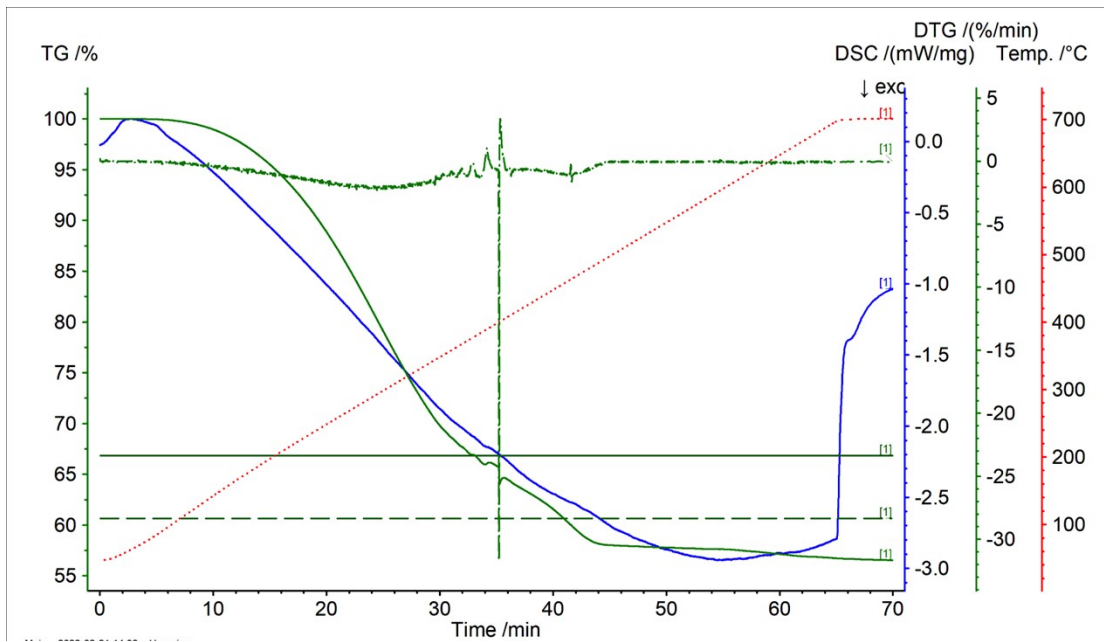
Figure S25: Thermo-gravimetric analysis (TGA) profile of the mixture of phytocat-2.5 and LDPE (1:10 by weight, Cycle 5)
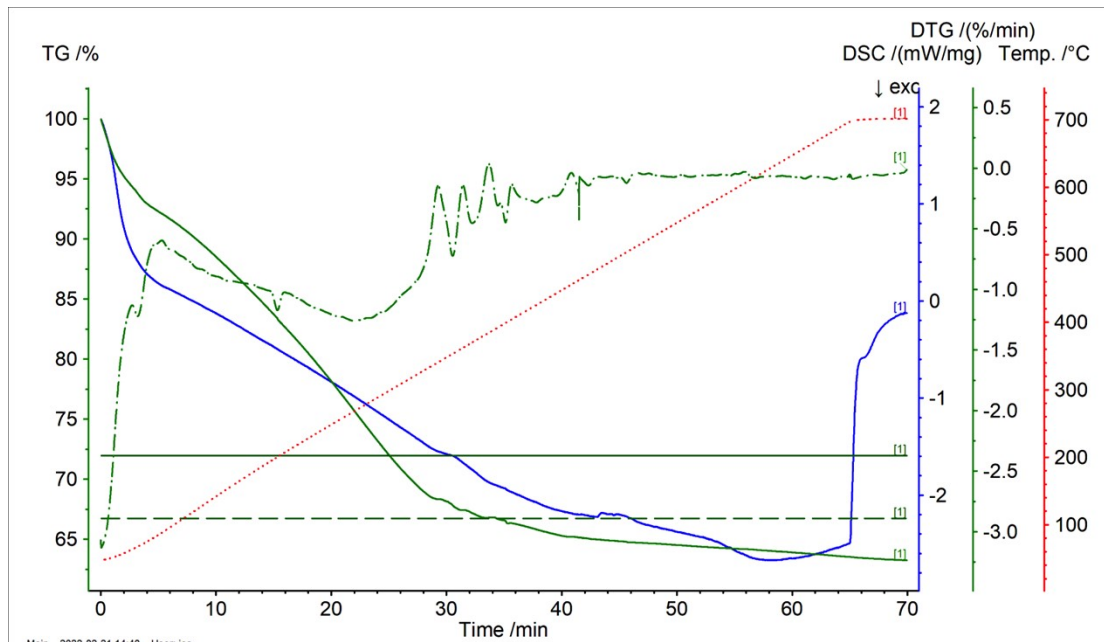
Figure S26: Thermo-gravimetric analysis (TGA) profile of the mixture of phytocat-2.5 and LDPE (1:10 by weight, Cycle 6)

**Supplementary Table 1:** Experimental results of the microwave-assisted depolymerization of polyethylene (Low density polyethylene, LDPE) using Ni-Phytocat-2.5 (varying catalyst: LDPE ratio by weight) at 250°C

| | (1:1) | (1:2) | (1:5) | (1:10) | (1:20) |
|---|---|---|---|---|---|
| Oil yield (wt%) | 31.0 | 43.0 | 54.0 | 60.7 | 54.9 |
| Solid yield (wt%) | 15.0 | 16.7 | 15.9 | 14.5 | 19.1 |
| Gas yield (wt%) | 54.0 | 40.3 | 30.1 | 24.8 | 19.5 |
| Oil composition (% Selectivity) | | | | | |
| **Mono-aromatics** | 31.9 | 21.2 | 20.1 | 34.2 | 19.2 |
| Benzene | 9.2 | 7.9 | 7.4 | 9.9 | 6.7 |
| Toluene | 15.1 | 9.5 | 9.2 | 16.7 | 7.9 |
| Xylene | 7.6 | 3.8 | 3.5 | 7.6 | 4.6 |
| **$C_6$-$C_{12}$ alkanes** | 11.1 | 9.2 | 7.9 | 9.1 | 2.5 |
| Octane | 2.4 | 1.5 | 0.9 | 2.7 | 0.5 |
| 1,2-dicyclopropyl ethane | 1.9 | 1.2 | 0.5 | 1.5 | 0.1 |
| Octyl-cyclopropane | 1.9 | 1.2 | 0.5 | 0.6 | 0.1 |
| Nonane | 2.1 | 1.9 | 0.9 | 1.1 | 0.4 |
| Decane | 1.5 | 0.4 | 0.9 | 1.5 | 0.4 |
| 2,4-Dimethyldecane | 0.9 | 0.2 | 0.5 | 0.4 | 0.5 |
| Undecane | 0.2 | 1.9 | 2.1 | 0.9 | 0.5 |
| Dodecane | 0.2 | 0.9 | 1.6 | 0.4 | 0.4 |
| **$C_6$-$C_{12}$ alkenes** | 29.0 | 27.4 | 25.6 | 32.7 | 16.7 |
| Octene | 7.4 | 6.5 | 4.9 | 9.2 | 3.3 |
| Nonene | 9.1 | 10.1 | 9.6 | 10.5 | 5.6 |
| Decene | 4.9 | 7.9 | 9.1 | 9.6 | 4.5 |
| 1-Tridecene | 4.1 | 1.1 | 0.1 | 1.1 | 2.2 |
| 1,9-Decadiene | 2.4 | 0.5 | 0.5 | 1.1 | 0.2 |
| 1,10-Undecadiene | 0.2 | 0.5 | 0.1 | 0.5 | 0.2 |
| 1-Undecene | 0.9 | 0.9 | 1.3 | 0.7 | 0.7 |

| | | | | | |
|---|---|---|---|---|---|
| **C$_{>12}$ alkanes** | 2.5 | 9.2 | 15.4 | 4.9 | 14.4 |
| Tridecane | 1.5 | 2.1 | 4.5 | 2.4 | 3.7 |
| Pentadecane | 0.5 | 2.5 | 2.7 | 1.1 | 2.9 |
| Hexadecane | 0.5 | 4.6 | 8.2 | 1.4 | 7.8 |
| **C$_{>12}$ alkenes** | 10.5 | 18.9 | 20.0 | 11.9 | 39.3 |
| 1,13-Tetradecadiene | 5.9 | 6.5 | 6.5 | 4.5 | 2.9 |
| 1,12-Tridecadiene | 1.5 | 2.5 | 5.5 | 2.0 | 6.5 |
| 1-Tridecene | 1.5 | 3.1 | 2.5 | 1.1 | 5.5 |
| Cetene | 0.5 | 2.5 | 2.3 | 1.5 | 4.9 |
| Octadecene | 0.5 | 1.5 | 1.5 | 0.1 | 2.0 |
| Eicosene | 0.5 | 1.5 | 1.1 | 0.5 | 9.5 |
| 1,19-Eicosadiene | 0.1 | 1.3 | 0.6 | 2.2 | 8.0 |
| **Poly-aromatics** | 15.0 | 14.1 | 11.0 | 7.2 | 7.9 |
| Indene | 2.5 | 2.4 | 2.5 | 1.5 | 2.0 |
| Naphthalene | 9.0 | 7.5 | 6.5 | 4.5 | 3.1 |
| Phenanthrene | 1.5 | 2.0 | 1.5 | 1.1 | 2.5 |
| Pyrene | 2.0 | 2.2 | 0.5 | 0.1 | 0.3 |
| Microwave energy consumption (KJ/g) | 36 | 54 | 24 | 12 | 44.4 |

**Supplementary Table 2:** Experimental results of the microwave-assisted de-polymerization of polyethylene (Low density polyethylene, LDPE) using Ni-Phytocat-2.5 (1:10, catalyst: LDPE by weight) for 6 successive cycles (each cycle takes t<70 s to reach the set-point of 250℃)

| | Cycle 1 | Cycle 2 | Cycle 3 | Cycle 4 | Cycle 5 | Cycle 6 |
|---|---|---|---|---|---|---|
| Oil yield (wt%) | 37.0 | 49.6 | 60.7 | 61.4 | 62.9 | 63.4 |
| Solid yield (wt%) | 31.1 | 24.5 | 14.5 | 14.6 | 15.2 | 15.9 |
| Gas yield (wt%) | 31.9 | 25.9 | 24.8 | 24.0 | 21.9 | 20.7 |
| Gas composition (% selectivity) | | | | | | |
| $H_2$ | 61.9 | 64.5 | 67.9 | 69.0 | 69.5 | 71.2 |
| $CH_4$ | 20.1 | 17.21 | 15.66 | 15.2 | 14.5 | 12.9 |
| CO | 0.37 | 0.48 | 0.64 | 0.71 | 0.79 | 0.92 |
| $CO_2$ | 0.14 | 0.14 | 0.32 | 0.39 | 0.42 | 0.46 |
| $C_{2-4}$ | 12.7 | 11.2 | 10.1 | 10.2 | 9.6 | 9.3 |
| Total conversion (%) | 68.9 | 75.5 | 85.5 | 85.4 | 84.8 | 84.1 |

**Supplementary Table 3:** Comparison of experimental results of the microwave-assisted (250℃, up to 2 min) and conventional thermal (500℃, up to 2 h) de-polymerization of polyethylene (Low density polyethylene, LDPE) using Ni-Phytocat-2.5 (1:10, catalyst: LDPE by weight)

| | Conventional | Microwave |
|---|---|---|
| Oil yield (wt%) | 67.5 | 60.7 |
| Solid yield (wt%) | 12.7 | 14.5 |
| Gas yield (wt%) | 19.8 | 24.8 |
| Oil composition (% selectivity) | | |
| Mono-aromatics | 6.5 | 34.2 |
| $C_5$-$C_{12}$ alkanes | 2.1 | 9.1 |
| $C_5$-$C_{12}$ alkenes | 39.3 | 32.7 |
| $C_{>12}$ alkanes | 11.9 | 4.9 |
| $C_{>12}$ alkenes | 8.1 | 11.9 |
| Poly-aromatics | 32.1 | 7.2 |
| Total conversion (%) | 87.3 | 85.5 |

**Supplementary Table 4:** Experimental results of the microwave-assisted de-polymerization of low density polyethylene (LDPE) using Ni-phytocat-0.1 (1:10, catalyst: LDPE by weight) for 3 successive cycles (each cycle took t<70 s to reach the set-point of 250℃)

|  | Cycle 1 | Cycle 2 | Cycle 3 |
|---|---|---|---|
| Oil yield (wt%) | 33.0 | 39.0 | 51.0 |
| Solid yield (wt%) | 39.0 | 34.9 | 25.9 |
| Gas yield (wt%) | 28.0 | 26.1 | 23.1 |
| Gas composition (% selectivity) |  |  |  |
| $H_2$ | 55.0 | 46.4 | 59.7 |
| $CH_4$ | 26.0 | 17.21 | 13.3 |
| CO | 0.33 | 1.15 | 2.45 |
| $CO_2$ | 0.22 | 1.56 | 0.97 |
| $C_{2-4}$ | 15.9 | 14.1 | 9.2 |
| Total conversion (%) | 61.0 | 65.1 | 74.1 |

**Supplementary Table 5:** Experimental results of the microwave-assisted de-polymerization of low density polyethylene (LDPE) using control-phytocat (1:10, catalyst: LDPE by weight) for 3 successive cycles (each cycle took t<70 s to reach the set-point of 250℃)

| | Cycle 1 | Cycle 2 | Cycle 3 |
|---|---|---|---|
| Oil yield (wt%) | 31.0 | 36.5 | 43.9 |
| Solid yield (wt%) | 45.5 | 39.5 | 33.9 |
| Gas yield (wt%) | 23.5 | 24.0 | 22.2 |
| Gas composition (% selectivity) | | | |
| $H_2$ | 51.0 | 43.2 | 40.4 |
| $CH_4$ | 27.2 | 22.7 | 18.4 |
| CO | 0.26 | 0.84 | 1.37 |
| $CO_2$ | 0.20 | 1.68 | 3.1 |
| $C_{2-4}$ | 16.7 | 19.1 | 18.3 |
| Total conversion (%) | 54.5 | 60.5 | 66.1 |

**Supplementary Table 6:** Experimental results of the microwave-assisted de-polymerization of low density polyethylene (LDPE) using activated carbon (1:10, catalyst: LDPE by weight) for 3 successive cycles (each cycle takes t<70 s to reach the set-point of 250℃)

| | Cycle 1 | Cycle 2 | Cycle 3 |
|---|---|---|---|
| Oil yield (wt%) | 34.0 | 37.0 | 45.5 |
| Solid yield (wt%) | 49.0 | 45.0 | 34.5 |
| Gas yield (wt%) | 17.0 | 18.0 | 20.0 |
| Gas composition (% selectivity) | | | |
| $H_2$ | 51.0 | 55.4 | 49.0 |
| $CH_4$ | 25.9 | 22.27 | 16.5 |
| $CO$ | 0.61 | 0.46 | 1.9 |
| $CO_2$ | 0.26 | 0.14 | 0.91 |
| $C_{2-4}$ | 15.6 | 15.0 | 16.9 |
| Total conversion (%) | 51.0 | 55.0 | 65.5 |

**Supplementary Table 7:** Comparison between literature reports on catalytic microwave assisted pyrolysis of plastics and this research

| Reference | Raw material | Temperature | Catalyst to plastic ratio | Oil yield | Oil composition |
|---|---|---|---|---|---|
| This work | LDPE | 250 °C | Phytocat: polymer = 1:1, 1:2, 1:5, 1:10, 1:20 | 31-61% (Ni-phytocat-2.5) 29-51% (Ni-phytocat-0.1) 33-42% (control phytocat) 34-49% (activated carbon) | Up to 97% $C \leq 23$, Up to 47% aromatics ( ~39% MAHs), Up to 42% $C_{<12}$ aliphatics (using Ni-phytocat-2.5) |
| 2 | HDPE | 400–600 °C | Activated carbon, ratio not given | 27.3–54.9% | >90% for $C \leq 21$, ~45–58% aliphatics; ~35–45% aromatics |
| 3 | HDPE | Not given | Tire/Carbon: plastic = ~1:3–2:1 | 43.9–83.9% | 38.73–88.37% aliphatics; only 6.61–17.31% aromatics |
| 4 | LDPE | 480 °C | ZSM-5: plastic = 1:4.68–1:1.32 | 24.44–32.58 wt% | >94% aromatics; 74.73–88.49% $C_8$-$C_{12}$ MAHs |
| 5 | LDPE | 375 °C | ZSM-5: plastic = 1:10 | 64.41 ± 5.20 wt% | 97% $C_8$-$C_{16}$ aromatics |
| 6 | LDPE | 350–550 °C | MgO: plastic = 1:15–1:3 | 24.2–38.5 wt% | 79.5–96.0% gasoline fraction; ~15–50% MAHs |

| Reference | Raw material | Temperature | Catalyst to plastic ratio | Oil yield | Oil composition |
|---|---|---|---|---|---|
| [7] | LDPE | 450–600 °C | NiO: HY: plastic = (1–5): 15:150 | 48.08–51.23 wt% | >92% $C_5$-$C_{12}$ gasoline fraction; 34.56–46.61% aromatics; 25.99–30.00% isomerized aliphatics |

| Reference | Raw material | Temperature | Catalyst to plastic ratio | Oil yield | Oil composition |
|---|---|---|---|---|---|
| [7] | LDPE | 450–600 °C | NiO: HY: plastic = (1–5): 15:150 | 48.08–51.23 wt% | >92% $C_5$-$C_{12}$ gasoline fraction; 34.56–46.61% aromatics; 25.99–30.00% isomerized aliphatics |

References

1    P. Johar, E. L. Rylott, C. R. McElroy, A. S. Matharu and J. H. Clark, *Green Chem.*, 2021, **23**, 808–814.

2    A. D. Russell, E. I. Antreou, S. S. Lam, C. Ludlow-Palafox and H. A. Chase, *RSC Adv.*, 2012, **2**, 6756–6760.

3    A. Undri, L. Rosi, M. Frediani and P. Frediani, *Fuel*, 2014, **116**, 662–671.

4    X. Zhang, H. Lei, G. Yadavalli, L. Zhu, Y. Wei and Y. Liu, *Fuel*, 2015, **144**, 33–42.

5    X. Zhang and H. Lei, *RSC Adv.*, 2016, **6**, 6154–6163.

6    L. Fan, Y. Zhang, S. Liu, N. Zhou, P. Chen, Y. Liu, Y. Wang, P. Peng, Y. Cheng and M. Addy, *Energy Convers. Manag.*, 2017, **149**, 432–441.

7    K. Ding, S. Liu, Y. Huang, S. Liu, N. Zhou, P. Peng, Y. Wang, P. Chen and R. Ruan, *Energy Convers. Manag.*, 2019, **196**, 1316–1325.